Contents lists available at www.goldenlightpublish.com/journals/jcemi/2-toc

Journal of Construction Engineering, Management & Innovation

Journal homepage: www.goldenlightpublish.com/journals/2/jcemi

Analytical design of RC–micropile connections in building underpinning

Antonio J. Sánchez-Garrido[1,*], Lorena Yepes-Bellver[2], Víctor Yepes[3]

[1] Universitat Politècnica de València, Department of Construction Engineering, Valencia, Spain
[2] Universitat Politècnica de València, Mechanics of Continuous Media and Theory of Structures Department, Valencia, Spain
[3] Universitat Politècnica de València, Institute of Concrete Science and Technology (ICITECH), Valencia, Spain

[*] Corresponding author: A. J. Sánchez-Garrido (ajsangar@doctor.upv.es)

https://doi.org/10.31462/jcemi.2026.725
Received 5 May 2026; Revised 22 June 2026; Accepted 6 July 2026; Available online 25 September 2026

Keywords

Construction technology
Micropile underpinning
Foundation retrofitting
Load transfer
Structural interfaces
Analytical framework

Abstract

The construction sector plays a key role in achieving global sustainability targets, making extending the service life of existing buildings a priority. In this context, micropile underpinning is widely used to restore the structural performance of foundations affected by severe geotechnical conditions. However, current structural and geotechnical standards provide limited and fragmented guidance for the analytical verification of load transfer mechanisms between micropiles and existing foundations. This study proposes a practical analytical framework to evaluate these connection interfaces through a two-interface decomposition of the load-transfer mechanism, by considering two governing mechanisms: (i) bond behavior between the steel casing and grout, and (ii) shear transfer between the grout and the existing concrete footing. The methodology is analytically verified through a full-scale underpinning project involving 158 micropiles, combining normative formulations, empirical approaches, and standardized pull-out test data. Results from the analyzed case study indicate that relying solely on the natural bond between smooth steel casings and conventional concrete joints results in a significant reduction in load transfer capacity, limiting it to approximately 15–20% of the theoretical structural capacity. In contrast, the use of welded corrugated connectors and high-performance expansive mortars significantly enhances interface capacity, allowing safe load transfer within practical geometric constraints. The study also provides a mechanical interpretation of how these solutions modify the internal strut-and-tie mechanism, improving stress distribution and reducing the risk of premature failure. These findings also highlight the potential of integrating the proposed analytical framework into digital design environments (e.g., BIM-based workflows), where interface-level verification could be incorporated as parametric checks to support decision-making in foundation retrofitting projects. The proposed framework offers a rational and practical basis for the design of micropile underpinning connections, contributing to more efficient and sustainable foundation retrofit solutions.

1. Introduction

The construction industry is increasingly recognized as critical in achieving the United Nations Sustainable Development Goals (SDGs). Buildings and infrastructure consume 36% of final energy and produce nearly 39% of global carbon dioxide emissions [1]. Within this sector, Portland cement production alone contributes to approximately 10% of global greenhouse gas emissions [2]. Consequently, transitioning from a linear "take-make-dispose" model towards circular economy strategies is imperative [3]. Extending the service life of existing buildings through structural rehabilitation reduces resource depletion, carbon emissions, and construction waste associated with demolition and new construction [4]. In parallel, the progressive digitalization of the construction sector, particularly through Building Information Modeling (BIM), is enabling more integrated approaches to lifecycle assessment and structural intervention planning, facilitating the incorporation of analytical verification procedures within data-rich design environments [5, 6].

Despite these environmental concerns, foundation elements remain among the least optimized components of building structures. From a lifecycle perspective, foundations are environmental hotspots that often account for over 20% of a building's embodied emissions, leading to over-engineered, unsustainable solutions [7, 8]. Recent studies have further highlighted that conservative assumptions in foundation retrofit design—particularly in deep foundation systems—can result in inefficient material use due to limited understanding of load transfer mechanisms [9, 10]. This limitation is consistent with recent experimental and multiscale investigations on deep foundation systems, which demonstrate that failure mechanisms are strongly governed by complex interactions between macro-scale stress redistribution and microstructural behavior at the soil–structure interface [11]. Structural design is fundamentally concerned with ensuring an efficient and safe transfer of loads from the superstructure to the ground. However, when competent soil is located at significant depth or is affected by severe geotechnical conditions—such as highly expansive clays—the feasibility of conventional shallow foundations is limited [12]. Under these challenging conditions, the rigid inclusion of micropiles to underpin the existing foundation has proven to be a reliable and globally adopted soil improvement procedure [13, 14].

Extensive geotechnical literature categorizes these deep foundation elements based on their grouting procedures, distinguishing between Global Unitary Injection (IGU) and Repetitive and Selective Injection (IRS), which significantly enhance the skin friction between the grout and the surrounding soil [15]. In standard engineering practice, designers typically optimize the foundation by matching the micropile's ultimate structural capacity (structural yield limit) to the soil's geotechnical bearing capacity. However, this conventional approach frequently neglects the internal mechanics of the connection node inside the existing footing. Recent experimental and analytical studies have emphasized the governing role of interface behavior in micropile systems, particularly regarding steel–grout bond and grout–concrete interaction mechanisms [16, 17]. The structural efficiency of the underpinning technique heavily relies on this vulnerable point, which must ensure the adequate transfer of internal forces from the column through the existing footing into the micropile. In practice, assessing the safety of this structural node involves solving a complex two-fold mechanical problem: first, defining the bond strength between the smooth tubular steel reinforcement and the surrounding cementitious grout (hereafter referred to as Interface 1); and second, determining the ultimate shear stress capacity of the connection between that grout and the existing concrete footing (hereafter referred to as Interface 2). These interfaces often govern the system's structural response and may control failure before the micropile reaches its geotechnical or structural capacity.

Despite the widespread use of micropiles, a significant gap persists in current design standards regarding the analytical justification of these confined connection nodes when micropiles act as rigid inclusions within existing foundations. Major international structural frameworks, such as the fib Model Code for Concrete Structures 2010 [18] and Eurocode 4 [19], as well as local guidelines, provide general, overly conservative adherence parameters but lack specific criteria for the strut-and-tie models applied to the confined nodes of micropiles. Because a micropile has a much smaller cross-section than a conventional pile, verifying the compression strut is highly critical. If the smooth steel tube is merely inserted into the footing, the compression strut is forced to transfer stresses through a reduced contact area, leading to high stress concentrations. The incorporation of mechanical connectors along the steel tube modifies this mechanism. It allows the compression strut to spread over a larger concrete area, resulting in a more uniform stress distribution. However, this effect is not explicitly considered in current design codes. This lack of explicit consideration reveals a fundamental gap: current standards do not provide a consistent analytical framework to verify the internal load-transfer mechanisms of micropile-to-footing connections under confined conditions. Consequently, in the absence of explicit regulatory guidance, the design must rely on technical guides and recommendations of a non-mandatory nature, which provide only indicative constructive solutions and are subject to engineering judgment rather than prescriptive compliance [20].

Regarding the grout-to-footing interface (Interface 2), standard design approaches based on concrete-to-concrete joints significantly limit the estimated shear capacity. For example, Article 47 of the Spanish EHE-08 code [21] defines the interface strength primarily as a function of the concrete tensile strength and a surface roughness factor, leading to highly conservative results. This normative approach heavily restricts the connection by making it exclusively dependent on a fraction of the concrete's design tensile strength, reduced by a minimal surface roughness factor. In the current Código Estructural [22], this formulation has not been directly replaced but incorporated into a more general framework. While theoretically more comprehensive, this transition has effectively complicated the verification process without providing specific guidance for confined foundation nodes such as micropile-to-footing connections. This lack of explicit criteria introduces significant uncertainty in design and often results in conservative or inconsistent solutions, a behavior also reflected in recent studies on interfacial shear mechanisms between new and existing concrete [23].

These highly conservative normative constraints contrast with widespread empirical approaches in geotechnical engineering. Methods proposed in SEMSIG-AETESS [24] or empirical formulas such as those developed by Serrano Alcudia [25] recognize practical resistances that systematically multiply these code limits by a factor of three or four. This discrepancy between empirical evidence and design standards highlights the absence of a consistent analytical framework for evaluating micropile-to-foundation connections under confined conditions.

To address this gap, this paper proposes an analytical framework for evaluating micropile-to-foundation connections. The methodology is validated through a real underpinning project involving 158 micropiles in a building affected by expansive soils. The study aims to answer two main research questions. First, whether the natural bond of smooth tubular steel is sufficient to transfer design loads safely, and whether mechanical connectors are required to ensure effective load transfer. Second, whether conventional concrete can provide adequate shear resistance at the grout-to-footing interface, or if the use of high-performance expansive mortars is necessary.

It must be emphasized that the objective of this study is not to provide full experimental validation, but to establish an analytically consistent and design-oriented framework grounded in existing normative formulations, empirical evidence, and standardized test data. The presented case study, therefore, serves as a full-scale application to demonstrate the internal coherence and practical applicability of the proposed methodology. Although the present study is not developed within a BIM environment, the proposed analytical framework is inherently compatible with digital modeling workflows, as it relies on parameterizable variables [5] that can be directly embedded into object-based structural models for enhanced traceability and verification.

2. Materials and Methods

The sustainable optimization of foundation substructures requires moving beyond purely empirical approaches toward analytically verifiable design procedures. In underpinning scenarios, the micropile often behaves as a rigid inclusion extending through most of the footing depth. Conventional design practice typically assumes that system capacity is governed by either the geotechnical bearing resistance or the steel tube's structural yield limit ($A_a \cdot fyd$). However, this assumption may overlook the influence of local load-transfer mechanisms within the confined connection node, which can control the structural response before these theoretical limits are reached. To analytically evaluate the internal load transfer mechanisms and ensure strict compliance with the Ultimate Limit State (ULS), the proposed framework decomposes the confined node into two critical interfaces, complemented by a global strut-and-tie verification of the existing footing. Within the proposed framework, normative formulations serve as lower-bound verification criteria to ensure compliance with Ultimate Limit State requirements, empirical approaches are used exclusively for contextual benchmarking, and an extrapolation-based method is introduced as a performance-based design alternative. This hierarchical structure ensures consistency between regulatory compliance and practical engineering applicability. This structured decomposition is particularly suitable for implementation within digital engineering environments, where each interface can be defined as a discrete verification object linked to geometric and material properties in a BIM-based model.

2.1. Structural limit state approach and scope definition

Before evaluating the adherence boundaries, the global stability of the connection node must be guaranteed. When rigid micropiles are installed through an existing footing, the foundation's structural behavior transitions to a rigid pile cap. Consequently, the existing footing must be analytically verified according to strut-and-tie models, such as Article 58.4.1.2 of the Spanish EHE-08 code [21].

This approach is consistent with internationally accepted design methodologies for discontinuity regions (D-regions), as formulated in Eurocode 2 [26] and the fib Model Code 2010 [18], ensuring that the adopted procedure is transferable beyond the Spanish regulatory framework. This verification ensures that the existing reinforcement is capable of resisting the multidirectional tensile forces (Td), which may be conservatively assumed equal in orthogonal directions (TdX = TdY) under symmetrical loading conditions.

Once the existing reinforcement is validated, the specific stress transfer mechanisms within the node must be assessed. To clarify this spatial configuration, Fig. 1 illustrates the structural arrangement of the confined underpinning node, including the governing geometric parameters and the compression strut associated with load transfer.

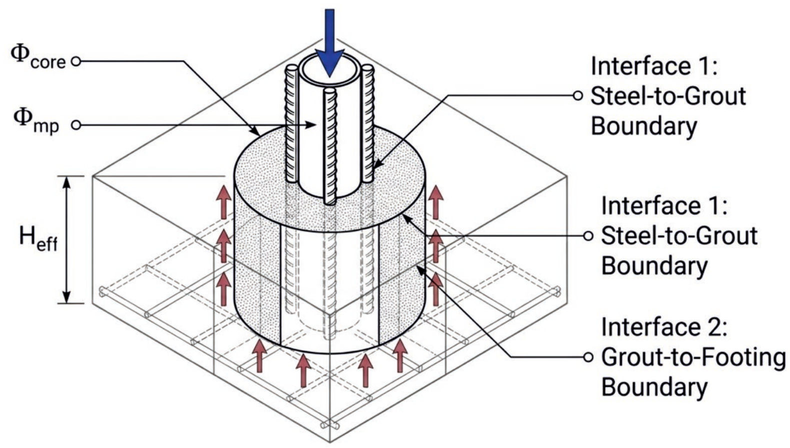

Fig. 1. Structural configuration and load transfer mechanism of the confined micropile underpinning node

Table 1 summarizes the analytical formulations considered in this study, including both normative and empirical approaches, which are subsequently evaluated within a unified verification framework. This culminates in the flowchart detailed in Fig. 2, which guides the ULS verification process for both the internal and external interfaces. Within this context, the proposed framework should be interpreted as an analytical verification methodology rather than an experimentally validated model, where normative formulations provide lower-bound safety criteria and experimental benchmarks are used to calibrate realistic interface behavior.

2.2. Mathematical modeling of Interface 1 (Steel-to-Grout)

Interface 1 evaluates the adherence between the tubular steel casing and the surrounding cementitious grout. Extensive literature establishes that the bond-slip behavior between steel and cementitious materials is a complex three-dimensional phenomenon fundamentally governed by three main resistant mechanisms: chemical adhesion, friction under lateral confinement, and mechanical interaction or wedging.

Because conventional smooth tubular steel casings entirely lack this crucial mechanical wedging, structural frameworks systematically penalize their capacity. Although obsolete from a regulatory standpoint, the EH-91 [27] formulation is retained in this study due to its explicit bond expressions, which are absent in more recent codes and provide a transparent analytical baseline for comparison. Specifically, Article 42.2 of the historical Spanish code EH-91 explicitly defines the ultimate design bond strength (τbd) for smooth bars strictly as a function of the characteristic compressive strength of the grout (fcm) divided by the concrete partial safety factor (γc=1.5), as expressed in Eq. (1):

Table 1. Summary of analytical formulations and governing mechanisms for the evaluation of micropile-to-foundation connection interfaces

Connection Boundary	Analytical Framework	Dominant Load Transfer Mechanism	Governing Code / Empirical Reference	Governing Equation for Ultimate Shear Stress (τru)
INTERFACE 1 (Steel-to-Grout)	Natural adherence	Chemical adhesion & friction	Spanish Code EH-91 (Art. 42.2)	Eq. (1)
	Natural adherence	Friction under confinement	Eurocode 4 (EN 1994-1-1)	Strictly capped at 0.55 MPa
	Advanced Concrete Code	Chemical adhesion on smooth steel	fib Model Code 2010 (Art. 6.1)	Evaluated analytically as ≈0.60 MPa
	Proposed Optimization	Mechanical wedging (ribs)	EH-91 (Corrugated bars)	Eq. (3)
INTERFACE 2 (Grout-to-Footing)	Concrete joint	Cohesion & surface roughness	Spanish Code EHE-08 (Art. 47.2)	Eq. (5)
	Empirical guidelines	Geotechnical consensus	SEMSIG-AETESS (2012)	Eq. (9)
	Empirical formula	Extrapolated crack observation	Serrano Alcudia (2005) formula	Eq. (10)
	Proposed Optimization	Volumetric expansion & High friction	Extrapolated UNE-EN 1881:2007	Derived from standardized pull-out tests

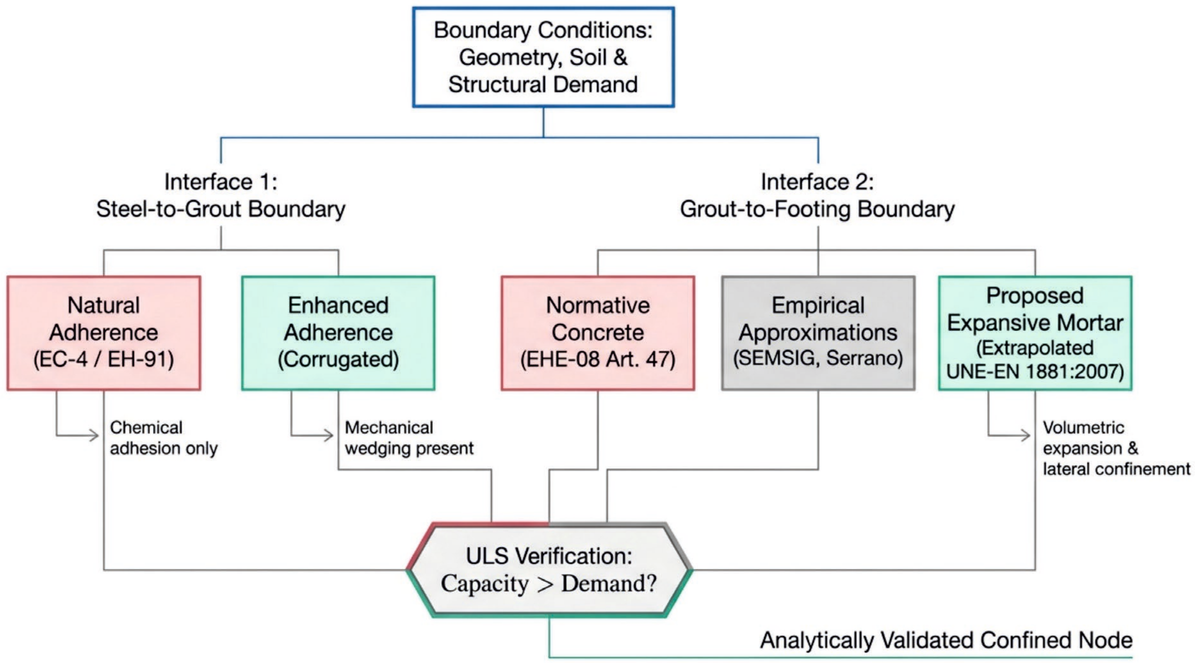

Fig. 2. Analytical flowchart for ULS verification of internal load transfer mechanisms in micropile underpinning systems

$$\tau_{bd} = (1.2/1.5)\sqrt{f_{cm}} \quad (1)$$

It must be strictly noted that this historical empirical formulation requires the characteristic compressive strength (f_{ck}) to be introduced in kg/cm², yielding an ultimate bond stress in kg/cm², which is subsequently converted to MPa for normative comparison purposes. Unless otherwise stated, all final stress values are expressed in MPa for consistency with current structural design frameworks.

Current frameworks like Eurocode 4 [19] are even more restrictive, limiting the ultimate shear stress (τ_{Rd}) for circular hollow sections filled with concrete to a mere 0.55 MPa, and for completely embedded sections to 0.30 MPa.

These limitations are consistent with international bond models for steel–concrete interfaces, where the absence of mechanical interlocking significantly reduces the transferable shear stress, as reflected in both Eurocode and fib Model Code provisions.

Mechanically, this lack of geometric interlocking exposes a critical flaw in the confined strut-and-tie model. Without wedging, the compression strut is forced to transfer stresses through a reduced contact area at the steel interface, leading to significant stress concentrations and increasing the risk of localized failure.

To overcome this structural bottleneck and physically alter the confined strut-and-tie model, the methodology evaluates the incorporation of welded corrugated steel connectors as a strategy to enhance load transfer capacity. Several longitudinal corrugated bars are welded to the tubular casing at equal intervals using continuous fillet welds. This configuration increases the effective load-transfer surface area and promotes a more uniform distribution of stresses in the surrounding concrete.

To mathematically quantify this structural enhancement, the methodology applies the specific formulation for corrugated bars defined in the same Article 42.2 of the EH-91 [27]. The design bond strength (τ_{bd}) is significantly increased by evaluating the ultimate bond failure stress (τ_{bu}), as defined in Eq. (2):

$$\tau_{bd} = (\tau_{bu}/1.6) \cdot (f_{cm}/225)^{2/3} \quad (2)$$

Where the ultimate bond failure stress (τ_{bu}) in kg/cm² is analytically defined according to Eq. (3), with ϕ_{rib} being the nominal diameter of the corrugated bar in millimeters:

$$\tau_{bu} = 130 - 0.9\phi_{rib} \quad (3)$$

To determine the design capacity of the mechanical connectors, the ultimate bond failure stress (τ_{bu}) is first converted into the design bond strength (τ_{bd}) by applying the corresponding partial safety factors, as defined in Eq. (2). τ_{bu} represents the ultimate bond capacity, while τbd corresponds to the design bond strength after applying safety factors. The resulting design bond strength is then multiplied by the effective bonding area of the corrugated connectors. This effective area should account for possible reductions due to welding seams or execution-related imperfections, which may be considered through an appropriate reduction factor. Finally, the total design resistance (R_d) is obtained as the product of the design bond strength and the effective contact area of all connectors.

2.3. Mathematical modeling of Interface 2 (Grout-to-Footing)

Interface 2 evaluates the structural resistance of the bond between the micropile grout and the internal surface of the existing concrete footing. This capacity is defined as the product of the contact surface (S) and the design shear stress ($\tau_{r,u}$) as defined by Eq. (4):

$$R_d = S \cdot \tau_{r,u} \quad (4)$$

The normative conflict arises when defining the τr,u parameter. If conventional concrete is considered to fill the connection node, the structural assessment must strictly comply with code provisions for shear friction in joints without transverse reinforcement. Following Article 47.2 of the EHE-08 [21], this highly conservative normative approach restricts the ultimate shear stress by making it exclusively dependent on a fraction of the concrete's design tensile strength ($f_{ct,d}$) reduced by a dimensionless surface roughness factor (β). This formulation establishes a strict lower bound that severely penalizes the theoretical capacity, as expressed in Eq. (5):

$$\tau_{r,u} = \beta\left(1.30 - 0.30\frac{f_{ck}}{25}\right) f_{ct,d} \geq 0.70\beta f_{ct,d} \quad (5)$$

For a typical structural concrete strength (f_{ck} = 25 MPa), commonly found in existing building stock, the mean tensile strength is calculated according to Eq. (6):

$$f_{ct,m} = 0.30 \cdot f_{ck}{}^{2/3} \quad (6)$$

The characteristic tensile strength is then obtained as:

$$f_{ct,k} = 0.70 \cdot f_{ct,m} \quad (7)$$

Applying a partial safety factor γ_c = 1.5 results in a design tensile strength of $f_{ct,d}$ = 1.20 MPa.

$$f_{ct,d} = f_{ct,k}/\gamma_c \quad (8)$$

When this value is introduced into Eq. (5), together with a realistic surface roughness factor (β = 0.3) characteristic of diamond core-drilled surfaces, the allowable shear stress is reduced to an impractically low value ($\tau_{r,u}$ = 0.36 MPa), while still respecting the normative lower bound (0.25 MPa).

For reference purposes, and to contextualize the magnitude of the obtained values within common engineering practice, the methodology also evaluates empirical formulations widely used in geotechnical applications. These formulations are not adopted as governing design criteria but are included to quantify the deviation between code-based predictions and observed in-situ behavior.

$$\tau_{r,u} = f_{ck}/20 \quad (9)$$

$$\tau_{r,u} = (0.9/1.6)\sqrt{f_{ck}/1.5} \quad (10)$$

These expressions correspond to the empirical recommendations of SEMSIG-AETESS [24] and the crack-based formulation proposed by Serrano Alcudia [25], respectively.

Since these empirical formulations are commonly used in engineering practice, the input variable f_{ck} must also be introduced in kg/cm², yielding an ultimate shear stress ($\tau_{r,u}$) in kg/cm². For this study, the resulting values have been mathematically converted to MPa (1.25 MPa and 0.73 MPa, respectively) to allow a direct comparison with current structural frameworks.

The comparison highlights that empirical estimates provide significantly higher interface capacities; however, because they lack explicit structural verification within ULS frameworks, they are not directly applicable for design purposes in the present methodology.

Because empirical approaches lack regulatory structural backing and the use of standard concrete evaluated through Eq. (5) leads to mathematically unfeasible designs and impractically large core drills, the proposed methodology evaluates the use of high-adherence, non-shrink expansive technical mortars (commercial high-performance non-shrink grouts) as a performance-based alternative to conventional solutions. These specialized cementitious products feature extreme compressive strengths (up to 70 MPa) and volumetric expansion properties that significantly increase lateral confinement, thereby enhancing the frictional component of the bond.

The proposed approach derives the interface capacity from standardized UNE-EN 1881:2007 [28] pull-out tests, extrapolated to the actual contact surface of the core drill. This extrapolation is adopted as a design-oriented estimation rather than a direct physical scaling. This distinction is necessary because the boundary conditions, stress distribution, and confinement levels in the standardized test differ from those in the real confined micropile–footing system. Therefore, this procedure should not be interpreted as a direct physical scaling law, but as a performance-based calibration strategy that translates experimentally validated interface behavior into a design-compatible parameter under confined conditions. Although scale effects may influence absolute stress values, the confined geometry of the micropile–footing system introduces higher lateral stresses that may partially compensate for these effects. However, this compensation is not explicitly quantified and remains an engineering approximation.

3. Case Study Description

To validate the proposed analytical methodology, an actual underpinning project is established as the reference case study. The project involves the structural rehabilitation of a two-story educational building (ground floor plus one) affected by severe geotechnical pathologies, specifically a low-bearing-capacity soil characterized by highly expansive clays and sulfate aggressiveness. The intervention required the execution of 158 micropiles, totaling 1235 linear meters, strategically distributed in groups of two or three units per isolated footing to control internal force redistribution within the foundation system. The selected case study is representative of typical foundation retrofit scenarios in expansive soils, where micropile underpinning is widely applied but where the structural verification of the connection node remains insufficiently addressed in current engineering practice [10].

3.1. Pathological context, macroscopic verification, and geometrical definition

The existing substructure, originally designed and constructed nearly two decades ago, consists of isolated reinforced concrete footings. Before assessing the localized stress transfer at the interfaces (as defined in Section 2), the global stability of the connection node had to be mathematically guaranteed. Because the original structural drawings were available, the exact geometry, concrete compressive strength, and steel reinforcement ratios of the existing footings could be determined with precision. Consequently, the existing footings were analytically verified as rigid pile caps (encepados rígidos) using strut-and-tie models, as required by Article 58.4.1.2 of the EHE-08 [21], in line with internationally recognized design principles for discontinuity regions [18]. Although plan dimensions and existing reinforcement ratios naturally varied across the different underpinning locations, all footings shared a constant total depth of 500 mm, which is the strictly governing geometric parameter for the localized interface evaluation. Preliminary macroscopic calculations confirmed that, in all cases, the existing bottom reinforcement provides sufficient capacity to resist the multidirectional tensile forces (TdX = TdY) generated by load transfer to the micropiles.

Geotechnical characterization based on site investigation reports identified highly plastic expansive clays with low bearing capacity, consistent with documented soil–structure interaction problems affecting shallow foundations [14]. Accordingly, the selection of micropile underpinning responds not only to structural requirements but also to the need to mitigate long-term volumetric soil effects.

Once the macroscopic stability of the footing was validated, the specific parameters of the rigid inclusions were defined. Table 2 summarizes the geometrical, mechanical, and structural parameters governing the existing foundation and the underpinning node, constituting the complete input dataset required for reproducibility of the analytical verification. The explicit definition of these parameters also facilitates their potential integration into digital models, enabling consistent data management and traceability within BIM-based representations of the existing structure and the underpinning intervention. It is worth noting that the effective thickness of the tubular casing (tef = 7.40 mm) accounts for a 0.60 mm sacrificial corrosion allowance, rigorously adopted in accordance with the Spanish Guidelines for the Design and Execution of Micropiles in Highway Works [20].

Table 2. Input parameters for the structural verification of the micropile-to-footing connection node

Structural Component	Parameter Description	Notation	Value	Unit
Existing Footing	Characteristic compressive strength	f_{ck}	25.00	MPa
	Mean / Characteristic tensile strength	$c_{t,m}$ / $f_{ct,k}$	2.56 / 1.80	MPa
	Concrete partial safety factor / Design tensile strength	γ_c / $f_{ct,d}$	1.50 / 1.20	- / MPa
	Total footing depth / Concrete cover	H / c	500.00 / 50.00	mm
	Theoretical / Executed core drill diameter	ϕ_{core}	150.00 / 170.00	mm
Tubular Steel Inclusion	Steel grade and design yield strength	f_{yd}	S-275 JR (275.00)	MPa
	Outer tubular casing diameter	ϕ_{mp}	88.90	mm
	Nominal / Effective thickness (accounting for 0.6 mm corrosion)	t / t_{ef}	8.00 / 7.40	mm
	Net steel cross-sectional area	A_a	1,894.70	mm²
	Effective embedment length	L_{ef}	450.00	mm
Connection Elements	Corrugated steel connectors (Diameter × Quantity)	ϕ_{rib}	16.00 × 3	mm × units
	Weld reduction factor / Effective bonding length	ρ_w / L_{weld}	0.75 / 337.50	- / mm
	Expansive technical mortar compressive strength	f_{cm}	69.30	MPa
Structural Demands	Maximum axial compression demand	N_d	376.00	kN
	Ultimate structural yield limit of the steel tube ($A_a \times f_{yd}$)	$R_{u,tube}$	521.04	kN

Fig. 3 illustrates the general layout and the standard cross-section of the underpinning intervention, detailing the geometric integration between the existing foundation and the new deep foundation elements. While the maximum axial compression demand (Nd) derived from the structural analysis is 376.00 kN, the theoretical ultimate structural capacity of the 8.0 mm thick steel tube reaches 521.04 kN, indicating that the governing condition of the system is the efficiency of the load transfer within the connection node rather than the structural resistance of the micropile itself. The case study is therefore treated as a deterministic validation scenario to assess the applicability of the proposed analytical framework under real construction conditions.

3.2. Execution sequence and quality control

Fig. 4 sequentially documents the execution phases of the underlying node, exposing the critical operations required to physically materialize the theoretical adherence capacities (τ_{bu} and $\tau_{r,u}$) at the interfaces.

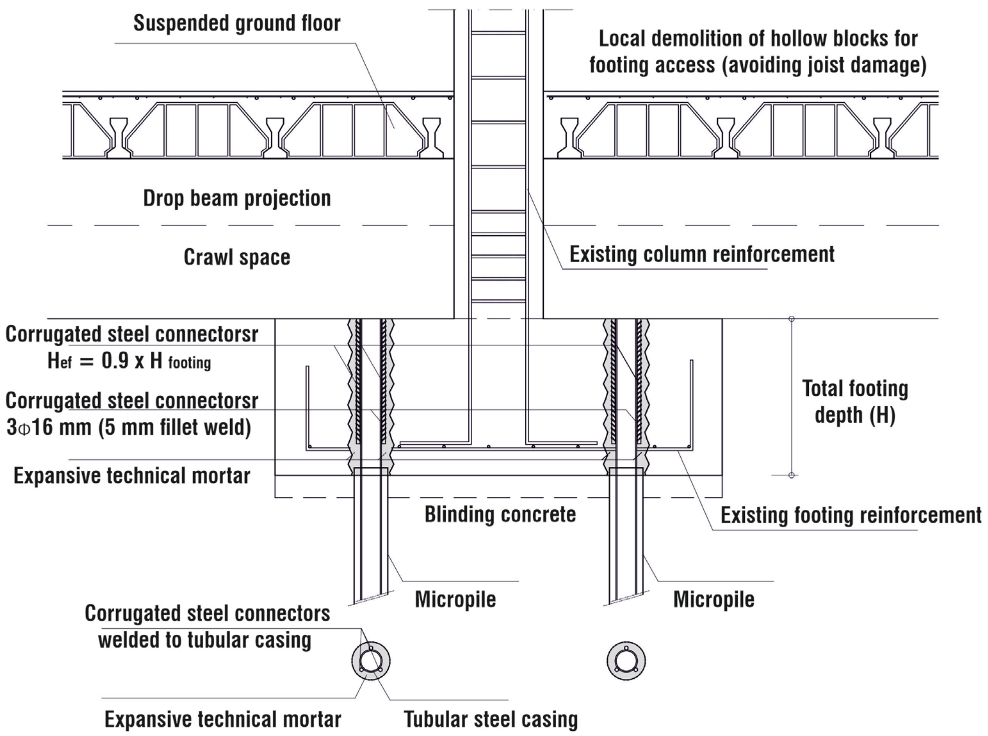

Fig. 3. General layout and representative cross-section of the micropile underpinning system and connection node configuration

Fig. 4. Sequential execution phases of the confined underpinning node: (a) Phase 1: Mechanical connector integration; (b) Phase 2: Core drilling and primary grouting; (c) Phase 3: High-pressure interface sanitization; (d) Phase 4: IRS grouting and expansive mortar confinement)

The construction procedure comprises four fundamental stages. First, corrugated steel connectors (B 500 S) are welded to the tubular casing (3ϕ16, length 450 mm) using continuous fillet welds, with the embedded length geometrically optimized to occupy 90% of the footing depth while preserving the required concrete cover. This detailing ensures consistent geometric conditions for load transfer along the interface.

Second, the existing footing is core-drilled, and the micropile is installed with primary grouting; however, this stage leaves residual debris and drilling mud adhering to the concrete surface, resulting in a degraded initial interface condition. Third, high-pressure water cleaning and extraction are applied to remove contaminants and restore the surface condition of the drilled concrete, which is necessary to enable effective mechanical interaction at the interface. Finally, the micropile is completed by cement grouting, and the connection zone is filled with high-adhesion, expansive technical mortar. For depths exceeding 5 m, the IRS method is employed [15] to enhance soil–grout interaction.

Strict quality control procedures were implemented throughout all stages to ensure consistency between design assumptions and execution, thereby minimizing uncertainties associated with construction variability and ensuring the reliability of the analytical validation.

4. Results and Discussion

The proposed analytical framework was applied to the case study to evaluate the load-transfer capacity of the confined underpinning node. The analysis evaluates whether the connection node can (i) reach the ultimate structural capacity of the steel tube ($R_{u,tube}$ = 521.04 kN) or (ii) safely transfer the design axial load (N_d = 376.00 kN), thereby identifying whether the governing condition is controlled by structural demand or interface limitations. This dual verification criterion allows distinguishing between demand-driven and intrinsically interface-limited mechanisms, in line with recent research emphasizing the critical role of local load-transfer mechanisms in micropile systems [9].

4.1. Quantitative assessment of the connection interfaces

4.1.1. Interface 1 (Steel-to-Grout): Overcoming the absence of mechanical wedging

The results summarized in Table 3 demonstrate that the natural adherence of smooth tubular steel is structurally insufficient under all normative frameworks considered. The EH-91 formulation yields a capacity of 158.97 kN (Capacity-to-Demand Ratio, CDR = 0.42), while the more restrictive provisions of Eurocode 4 [19] reduce this value to 69.12 kN (CDR = 0.18). Even under the fib Model Code 2010 [18] assumptions, the interface capacity remains limited to 75.41 kN (CDR = 0.20). These results confirm that adhesion and friction alone cannot mobilize the required load transfer, particularly in confined conditions where early bond degradation governs the response, as also observed in steel–grout and composite interface studies [29].

The integration of welded corrugated connectors introduces mechanical interlocking. This modification increases the effective load-transfer area and reduces stress concentration at the steel–grout interface. However, for practical, conservative design verification, combining the mechanical contribution (394.17 kN) with the baseline natural adherence provided by the fib Model Code 2010 (75.41 kN) yields a conservative estimate of the total interface resistance. The bond supports this assumption–slip behavior of steel–cementitious interfaces, in which adhesion governs the initial elastic response. At the same time, mechanical interlocking controls the post-slip resistance, allowing both mechanisms to act sequentially and partially in parallel. This additive approach is adopted as a conservative approximation, assuming that adhesion primarily contributes in the pre-slip regime. At the same time, mechanical interlocking governs the post-slip response, thereby avoiding double-counting of resisting mechanisms.

Table 3. Analytical capacity breakdown and structural verification of Interface 1 (Steel-to-Grout)

Analytical Approach	Contact Area / Connectors Evaluated	Calculated Unitary Shear Stress (τ)	Derived Load Capacity (R_d)	CDR (R_d/N_d)	CYR ($R_d/R_{u,tube}$)	Verification Status
Natural Adherence (EH-91)	Smooth steel tube (125,680 mm²)	1.26 MPa (τ_{bd})	158.97 kN	0.42	0.30	Insufficient
Natural Adherence (Eurocode 4)	Smooth steel tube (125,680 mm²)	0.55 MPa (τ_{Rd})	69.12 kN	0.18	0.13	Insufficient
Natural Adherence (fib MC2010)	Smooth steel tube (125,680 mm²)	0.60 MPa (τ_{bd})	75.41 kN	0.20	0.14	Insufficient
Mechanical Connectors Contribution	3ϕ16 mm (L_{weld} =337.5 mm/bar)	11.56 MPa (τ_{bu})	394.17 kN	1.05	0.76	N/A
TOTAL PROPOSED DESIGN	fib MC2010 + Corrugated Connectors	-	469.58 kN	1.25	0.90	Verified / Safe

Note: CDR evaluates safety against the design load (N_d=376.00 kN). CYR evaluates the interface against the ultimate structural limit of the steel tube ($R_{u,tube}$=521.04 kN).

Although insufficient on its own, the baseline adhesion is conservatively retained as a secondary contribution acting in parallel with the mechanical interlocking mechanism. As detailed in Table 3, this combined approach safely justifies a total verified capacity of 469.58 kN, achieving CDR = 1.25 and CYR (Capacity-to-Yield Ratio) = 0.90. This transition from adhesion-controlled to mechanically controlled behavior is consistent with experimental evidence showing that roughened or ribbed interfaces significantly enhance bond strength and delay slip-induced degradation [10]. Furthermore, similar improvements in bond mobilization due to mechanical interlock have been reported in grout–concrete systems, where surface morphology governs post-peak resistance [30].

From a structural perspective, the results indicate that once mechanical interlocking is activated, Interface 1 no longer governs the critical condition under the analyzed conditions, shifting it toward the external boundary. This observation aligns with broader findings in micropile behavior, where connection detailing becomes decisive once axial capacity is sufficiently high [16].

4.1.2. Interface 2 (Grout-to-Footing)

The evaluation of Interface 2 reveals a significant discrepancy between normative predictions and experimentally achievable capacities. The analytical results are detailed in Table 4. They are comparatively illustrated in Fig. 5, where the capacities derived from different approaches are benchmarked against both the maximum axial demand (Nd = 376.00 kN) and the ultimate structural requirement (Ru,tube = 521.04 kN).

Under the strict application of EHE-08 (Eq. 5), the resulting shear stress (τr,u = 0.36 MPa) leads to a capacity of only 96.13 kN for the executed Ø170 mm core (CYR = 0.18). As shown explicitly in Table 4, satisfying the structural demand with this formulation would require a theoretical drill diameter of 921.4 mm, which is impractical and incompatible with typical footing geometries.

Table 4. Analytical capacity breakdown of Interface 2 (Grout-to-Footing) demonstrating the normative gap and the theoretically required drill diameter to satisfy the ultimate structural limit (521.04 kN)

Analytical Framework	Underlying Variables and Assumptions	Calculated Unitary Shear Stress (τ_{ru})	Derived Capacity for executed ϕ170 mm (R_d)	CYR ($R_d/R_{u,tube}$)	Required Contact Area (mm²)	Theoretically Required Drill Diameter (ϕ_{req})
Spanish Code EHE-08 (Art. 47)	Concrete joint (β=0.3, $f_{ct,d}$=1.20 MPa)	0.36 MPa	96.13 kN	0.18	1,447,333	921.4 mm (Unfeasible / Destructive)
Empirical Formula (Serrano)	Empirical crack assessment observation	0.726 MPa	193.86 kN	0.37	717,686	456.9 mm (Severely oversized)
Geotech. Guidelines (SEMSIG)	Empirical engineering consensus	1.25 MPa	333.79 kN	0.64	416,832	265.4 mm (Oversized)
PROPOSED OPTIMIZATION (UNE-EN 1881 Extrapolation)	Volumetric expansion & High friction	2.10 MPa	560.77 kN	1.08	248,114	157.9 mm (Optimum / Executed ϕ170 mm)

Note: Theoretical calculations assume a constant existing footing depth (H=500 mm). Values expose the unfeasible geometrical requirements of conventional frameworks.

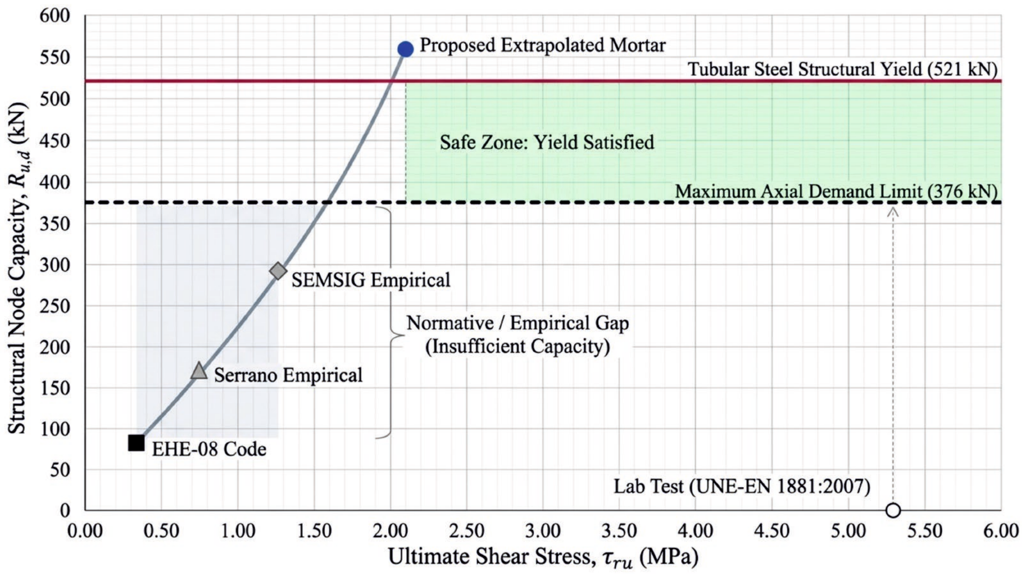

Fig. 5. Comparative bar chart of the ultimate load capacities evaluated through normative, empirical, and proposed methods against the maximum structural demand

Empirical approaches partially alleviate this limitation but remain insufficient. Serrano Alcudia's formulation increases the capacity to 193.86 kN, while the SEMSIG-AETESS guideline reaches 333.79 kN. However, as evidenced in Fig. 5, neither approach achieves the required structural threshold, confirming that empirical rules alone do not guarantee full load transfer under the analyzed conditions.

The proposed methodology, based on extrapolating UNE-EN 1881 pull-out tests, provides a rational estimate of interface capacity, though it relies on assumptions about scale effects and confinement conditions. The results of its application yield a design shear stress of 2.10 MPa, resulting in a capacity of 560.77 kN (CYR = 1.08). As shown in Table 4 and the final bar of Fig. 5, this value not only satisfies the maximum axial demand but also exceeds the ultimate structural capacity of the steel tube. This demonstrates that the combined effect of high-strength mortar and confinement-driven friction provides a consistent alternative to normative formulations without resorting to excessive geometric enlargement. Comparable trends have been reported in experimental studies, where interface shear capacity increases significantly with confinement and grout quality [30, 31].

4.2. Qualitative discussion and practical implications

The results confirm that the confined underpinning node behaves as a critical structural discontinuity region (D-region), where failure is controlled by local interface mechanics rather than global geotechnical or structural capacity. This behavior is consistent with recent numerical and experimental studies highlighting the dominant role of local load-transfer mechanisms in micropile-supported systems [9]. This interpretation is further supported by recent research showing that failure mechanisms in deep foundation systems emerge from coupled macro-scale stress paths and microstructural interactions [11], reinforcing the need for multiscale analytical approaches in confined structural nodes.

At Interface 1, the inability of smooth tubular steel to develop sufficient bond is directly associated with the absence of mechanical interlocking. Without ribs or connectors, load transfer is limited to chemical adhesion and friction, which degrade rapidly with minimal slip, preventing the formation of a stable compression strut within the footing. As illustrated in Fig. 6a, this results in stress concentration over a reduced contact perimeter. The introduction of corrugated connectors (Fig. 6b) modifies this internal load-transfer mechanism by expanding the effective contact perimeter and promoting the development of a wider compression strut over a larger concrete prism. This produces a more homogeneous stress distribution and mitigates stress concentrations at the steel–concrete interface, in agreement with bond-slip behavior reported in experimental studies on textured and ribbed interfaces [10, 29].

At Interface 2, standard code formulations, such as EHE-08, are based on conservative shear-friction models that primarily account for cohesion and surface roughness, which are intentionally formulated to ensure safety across a wide range of structural applications. However, as shown in Table 4 and Fig. 5, this simplification results in a severe underestimation of the actual capacity. Experimental evidence indicates that confinement stress significantly enhances frictional resistance and delays interface failure [31], while recent multiscale analyses confirm the strong dependency of interfacial shear strength on confinement and microstructural interaction [23]. In line with these findings, recent coupled experimental–microstructural studies have demonstrated that confinement-induced strength gains are intrinsically linked to microstructural evolution and stress redistribution mechanisms within deep foundation systems [11].

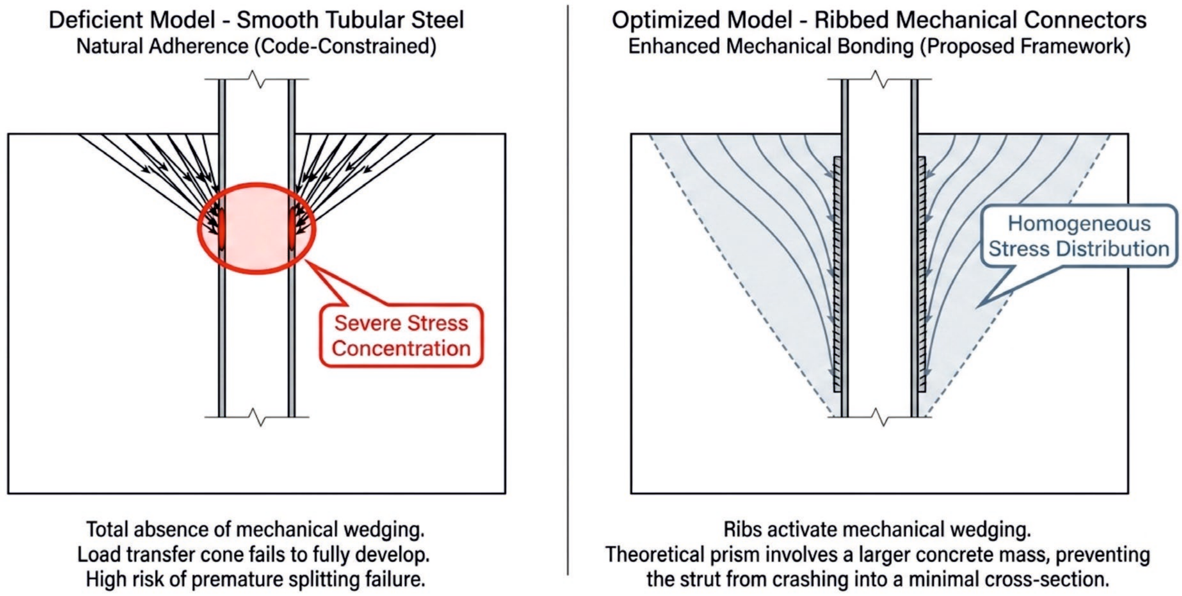

Fig. 6. Conceptual strut-and-tie mechanical model within the existing footing. (a) Stress concentration and premature failure risk on a smooth tubular casing; (b) Homogeneous stress distribution and load transfer cone development achieved through the integration of welded mechanical connectors

However, the exact quantification of confinement-induced stress amplification is not explicitly addressed in this study and is implicitly incorporated within the calibrated design shear stress derived from experimental benchmarks.

In the proposed solution, the use of expansive technical mortars generates active radial pressure against the core-drilled concrete surface, increasing the normal stress at the interface and, consequently, the mobilized shear capacity. The extrapolation procedure summarized in Table 5 provides a consistent link between laboratory testing and in-situ behavior, allowing the interface capacity to be derived from experimentally validated parameters. This approach replaces empirical assumptions with performance-based design, aligning with emerging trends in advanced structural assessment. From a digital engineering perspective, this approach could be incorporated into BIM-based decision-support systems [5, 6], where analytical verification of interface behavior is linked to construction detailing and material specifications, improving coordination between design and execution phases.

From a practical standpoint, the combined optimization of both interfaces allows the designer to replace traditional overdimensioning strategies with mechanically driven design optimization.

Table 5. Experimental extrapolation of the expansive technical mortar pull-out test (UNE-EN 1881:2006) for Interface 2 optimization

Extrapolation Step	Parameter Description	Standardized Laboratory Sample (UNE-EN 1881)	In-situ Case Study Extrapolation
1. Geometric Baseline	Drill diameter (ϕ)	30.00 mm	170.00 mm (ϕ_{core})
	Embedment depth (H)	150.00 mm	500.00 mm
	Effective Contact Area (S)	14,137.00 mm²	267,036.00 mm²
2. Laboratory Validation	Reference Testing Load	Minimum 75.00 kN (displacement < 0.6 mm)	-
	Tested Confined Shear Stress	5.30 MPa (tested without failure)	-
3. Safety Integration	Commercial Baseline Validation	-	3.00 MPa (Guaranteed threshold by commercial high-performance expansive grouts)
	Derived Design Shear Stress (τ_{ru})	-	2.10 MPa (Incorporating a partial safety factor for material and in-situ execution uncertainties ($\gamma_m \approx 1.45$), translating the guaranteed 3.00 MPa to a design value of 2.10 MPa)
4. Final Verification	Ultimate Extrapolated Capacity (R_d)	-	560.77 kN
	Verification Status (CYR = 1.08)	-	Verified / Safe (560.77 kN > 521.04 kN)

Note: The methodology derives the ultimate capacity by escalating standardized laboratory data to the executed oversized 170 mm core drill, incorporating market-based safety thresholds.

As shown in Table 4, increasing the drill diameter alone yields impractical solutions, whereas integrating mechanical connectors and high-performance mortars achieves the required capacity within feasible geometric limits. This approach not only ensures structural safety but also reduces material consumption, contributing to more sustainable foundation solutions in line with current research on low-impact construction systems [7, 14].

4.3. Limitations of the study and future research lines

Despite the robustness of the proposed analytical framework, certain limitations must be acknowledged. The capacity of Interface 2 is derived from the extrapolation of standardized pull-out tests, which do not fully replicate the boundary conditions of a confined micropile node at full scale. Scale effects, three-dimensional confinement, and construction-induced variability may influence the actual stress distribution. The extrapolation approach introduces uncertainty due to scale effects and confinement conditions, potentially leading to deviations in the estimated shear capacity. These uncertainties should be quantified in future studies through controlled experimental validation, particularly through parametric analyses that explicitly assess the influence of scale effects, confinement conditions, and construction variability on the resulting interface capacity. Recent studies have emphasized that such uncertainties are closely linked to the interaction between microstructural phenomena and global stress redistribution, underscoring the need for integrated experimental and multiscale modeling approaches to capture failure mechanisms in deep foundation systems accurately [11].

Additionally, the performance of the proposed solution is inherently dependent on construction quality, including surface preparation, welding execution, and proper placement of expansive mortar. Variability in these processes may significantly affect the actual interface capacity, and this execution-dependent uncertainty is not explicitly quantified in the current analytical model. Furthermore, the analysis focuses on bond- and shear-failure mechanisms at the interfaces. In contrast, other potential failure modes, such as local concrete splitting, punching effects, or weld failure, are not explicitly evaluated and should be considered in a comprehensive structural assessment.

The proposed framework is sensitive to key input parameters, including surface roughness factors, material strengths, connector geometry, and execution-related reduction factors. A formal parametric or sensitivity analysis is not included in the present study; therefore, the model's robustness under varying conditions should be further investigated in future research. Such studies should also include full-scale experimental testing and calibrated nonlinear finite-element simulations to quantify the influence of confinement and to validate the proposed analytical assumptions. These approaches would provide a deeper understanding of failure mechanisms and help develop more accurate, internationally applicable design guidelines. Future developments could also explore integrating the proposed methodology into BIM-based platforms, enabling automated verification workflows and reducing uncertainty associated with manual data handling. These digital integration strategies, lean management frameworks, and advanced lifecycle assessment workflows align closely with recent sustainability innovations highlighted in construction engineering practices [32−34]. However, such implementation falls outside the scope of the present study.

It must be explicitly noted that the objective of this study is not to provide a full experimental validation of the proposed framework, but rather to establish an analytically consistent and design-oriented methodology grounded in existing normative formulations, empirical evidence, and standardized test data. The presented case study, therefore, serves as a deterministic application scenario to demonstrate the approach's internal coherence and practical applicability, rather than as an independent experimental validation dataset.

5. Conclusions

This study presents an analytical framework for the structural verification of confined micropile underpinning nodes, focusing on internal load-transfer mechanisms. The application to the case study confirms that the structural response of the system is governed not by the global geotechnical capacity or the axial resistance of the micropile, but by the weakest adherence interface within the connection node.

The results show that the structural response is governed by interface behavior rather than global capacity. Within the context of the analyzed case study, the results indicate that the natural bond of smooth tubular steel is insufficient to safely transfer design loads, thereby requiring the incorporation of mechanical connectors, and that conventional concrete joints do not provide adequate shear resistance at the grout-to-footing interface without the use of high-performance expansive mortars. This limitation is directly associated with the absence of mechanical interlocking, which confines load transfer to adhesion and friction mechanisms that degrade rapidly under minimal slip. The incorporation of welded corrugated connectors overcomes this limitation by modifying the internal force transfer mechanism, enabling the development of a stable compression strut and allowing the interface to reach capacities compatible with the structural demand.

For the grout-to-footing interface, code-based formulations yield conservative estimates that lead to impractical geometries. The results indicate that confinement effects play a key role in increasing shear capacity when high-performance mortars are used. The extrapolation of standardized pull-out test results to the real geometry of the connection node is proposed as a viable strategy to bridge the gap between normative limitations and actual material behavior. This approach provides a rational, reproducible, and design-oriented basis for evaluating interface capacity, enabling the direct incorporation of experimentally validated performance parameters into analytical verification frameworks and reducing reliance on purely empirical assumptions.

From a practical perspective, the proposed methodology demonstrates that the optimization of underpinning systems should be driven by interface mechanics rather than geometric overdimensioning. By ensuring that both internal boundaries of the node can mobilize the required load transfer, the design can achieve structural safety, reduce unnecessary material use, and improve construction efficiency. Although the study is framed within the context of Spanish and European regulations, the proposed methodology is based on fundamental mechanical principles. It can be adapted to other international design contexts, provided that local material and safety factors are properly considered. The presented results should be interpreted as an analytical validation of the proposed framework through a real-scale application, rather than as an independent experimental validation. Further research, including controlled full-scale testing and numerical simulations, is required to quantify the influence of confinement and scale effects.

Declarations

Conflict of Interests

The author(s) declared no potential conflicts of interest with respect to the research, authorship, and/or publication of this article.

Funding

Grant PID2023-150003OB-I00 funded by MICIU/AEI/10.13039/501100011033 and by “ERDF/EU”.

Author Contributions

A. J. Sánchez-Garrido: Conceptualization, Methodology, Software, Formal analysis, Investigation, Validation, Writing-Original draft. L. Yepes-Bellver: Supervision, Writing-Review & Editing. V. Yepes: Funding acquisition, Supervision, Writing-Review & Editing. All authors have read and agreed to the published version of the manuscript.

Acknowledgments

The authors would like to thank “GeoStrucTech S.L.” for providing some of the data and geotechnical information needed for this study.

Data Availability Statement

No new data were created or analyzed in this study.

Ethics Committee Permission

Not applicable.

Use of Generative AI and AI-assisted Technologies

During the preparation of this work, the authors used language editing tools solely for proofreading and text polishing, and have thoroughly reviewed and approved the final content.

References

[1] IEA (2021) Net Zero by 2050. https://www.iea.org/reports/net-zero-by-2050.

[2] Lehne J, Preston F (2018) Making concrete change – Innovation in low-carbon cement and concrete. The Royal Institute of International Affairs. ISBN 978-1784132729.

[3] Long W, Ng ST, Lu W, Mora L, Bao Z (2025) Deciphering how digital functions enable circular economy practices in construction: A critical review of recent progress and future outlook. Environ Impact Assess Rev 113:107889. https://doi.org/10.1016/j.eiar.2025.107889.

[4] Schöggl J-P, Stumpf L, Baumgartner RJ (2020) The narrative of sustainability and circular economy - A longitudinal review of two decades of research. Resour Conserv Recycl 163:105073. https://doi.org/10.1016/j.resconrec.2020.105073.

[5] Kang J, Liu Y, Wang Y (2026) BIM reverse modeling and performance optimization for low-carbon retrofitting of existing buildings powered by smart construction. Civil Engineering and Smart Structure Technology. https://doi.org/10.3233/ATDE251658.

[6] Zou X, Tan Y, Zhang G, Hou L (2026) BIM-based sustainability analysis for building green retrofit: A systematic review. Energy Build 354:116982. https://doi.org/10.1016/j.enbuild.2026.116982.

[7] Pujadas-Gispert E, Sanjuan-Delmas D, De la Fuente A, Moonen SPG, Josa A (2020) Environmental analysis of concrete deep foundations: Influence of prefabrication, concrete strength, and design codes. J Clean Prod 244:118751. https://doi.org/10.1016/j.jclepro.2019.118751.

[8] Sánchez-Garrido AJ, Moreno-Serrano JF, Navarro IJ, Yepes V (2026) Innovative safety framework and direct load–settlement method to optimize vertical subgrade modulus in sustainable mat foundations. Environ Impact Assess Rev 118:108191. https://doi.org/10.1016/j.eiar.2025.108191.

[9] Ebadi-Jamkhaneh M, Kontoni DPN (2023) Numerical investigation of micropile–raft systems under vertical loading. Innov Infrastruct Solut 8:76. https://doi.org/10.1007/s41062-023-01076-y.

[10] Elsawwaf M, Nazir A, El Naggar H (2023) Behavior of micropiles used in underpinning existing structures. Buildings 13(2):422. https://doi.org/10.3390/buildings13020422.

[11] Zhou Z, Yepes-Bellver L, Alcalá J, Yepes V (2025) Study on the failure mechanism of deep foundation pit of high-rise building: Comprehensive test and microstructure coupling.

Buildings 15(8):1270. https://doi.org/10.3390/buildings15081270.

[12] Yepes V (2020) Procedimientos de construcción de cimentaciones y estructuras de contención, 2ª ed. Colección Manual de Referencia, Universitat Politècnica de València, 480 pp. ISBN 978-84-9048-903-1.

[13] Mollaali M, Alitalesh M, Yazdani M, Shafie MB (2014) Soil improvement using micropiles. In: 8th European Conference on Numerical Methods in Geotechnical Engineering (NUMGE): Numerical Methods in Geotechnical Engineering, vol. 1. Delft University of Technology, Delft, Netherlands, pp. 535–540, 18–20 Jun 2014.

[14] Sánchez-Garrido AJ, Navarro IJ, Yepes V (2022) Evaluating the sustainability of soil improvement techniques in foundation substructures. J Clean Prod 351:131463. https://doi.org/10.1016/j.jclepro.2022.131463.

[15] Bustamante M (1986) Un método para el cálculo de los anclajes y de los micropilotes inyectados. Bol Inf Lab Carreteras 174:3–23.

[16] Pellicer-Martínez F, Martínez-Lirón V, Hernández-Díaz AM, Pérez-Aracil J, López-Juárez JA (2023) The Economic Impact Associated with the Direct Connection Strength of Micropiles in Foundation Retrofit Projects. Buildings 13(4):980. https://doi.org/10.3390/buildings13040980.

[17] Martínez-Lirón V, Pellicer-Martínez F, Hernández-Díaz AM, Abellán-García J (2025) Toward efficient foundation reinforcement: Introducing the hat direct connection method for efficient micropile underpinning systems. Structures 77:109203. https://doi.org/10.1016/j.istruc.2025.109203.

[18] Fédération internationale du béton (fib) (2012) fib Model Code for Concrete Structures 2010. Ernst & Sohn. https://www.fib-international.org/publications/fib-bulletins/model-code-2010-final-draft%2C-volume-1-detail.html.

[19] Comité Europeo de Normalización (CEN) (2004) EN 1994-1-1: Eurocode 4: Design of composite steel and concrete structures – Part 1-1: General rules and rules for buildings. CEN. https://cdn.transportes.gob.es/portal-web-transportes/carreteras/normativa_tecnica/21_eurocodigos/AN_UNE-EN-1994-1-1.pdf.

[20] Ministry of Public Works (2005) Guía para el proyecto de ejecución de micropilotes en obras de carretera. Ministerio de Fomento. Dirección General de Carreteras [in Spanish]. https://www.transportes.gob.es/recursos_mfom/0710200.pdf.

[21] Ministry of Public Works (2008) Instrucción del Hormigón Estructural (EHE-08) [in Spanish]. https://www.transportes.gob.es/recursos_mfom/1820100.pdf.

[22] Ministry of Transport, Mobility and Urban Agenda (2021) Código Estructural [in Spanish]. https://www.boe.es/eli/es/rd/2021/06/29/470/dof/spa/pdf.

[23] Huang H, Jiang B, Guo T, Fang M, Wang T, Tu Y, Ji Y, Wang C, Sas G (2025) New insights into the interfacial shear behavior of new-to-old concrete: A molecular dynamics simulation study. Constr Build Mater 140:140691. https://doi.org/10.1016/j.conbuildmat.2025.140691.

[24] Asociación de Empresas de la Tecnología Suelo y Subsuelo (AETESS) (2012) Recalces con micropilotes y otras técnicas especiales [in Spanish] (Jornadas Técnicas SEMSIG-AETESS, 12.ª sesión). AETESS. ISBN 978-84-695-3911-8.

[25] Serrano Alcudia F (2005) Patología de la edificación: El lenguaje de las grietas. ISBN 978-84-86957-90-2.

[26] Comité Europeo de Normalización (CEN) (2004) EN 1992-1-1: Eurocode 2: Design of concrete structures – Part 1-1: General rules and rules for buildings. CEN. https://cdn.mitma.gob.es/portal-web-drupal/carreteras/normativa/AN_UNE-EN%201992-1-1.pdf.

[27] Ministry of Public Works and Transport (1991) Instrucción para el proyecto y la ejecución de obras de hormigón en masa o armado (EH-91) [in Spanish]. https://www.boe.es/eli/es/rd/1991/06/28/1039.

[28] AENOR (2007) UNE-EN 1881:2007. Productos y sistemas para la protección y reparación de estructuras de hormigón. Métodos de ensayo. Ensayo de los productos de sellado del anclaje por el método del arrancamiento. Asociación Española de Normalización y Certificación.

[29] Veludo J, Dias-da-Costa D, Júlio ENBS, Pinto PL (2012) Bond strength of textured micropiles grouted to concrete footings. Eng Struct 35:288–295. https://doi.org/10.1016/j.engstruct.2011.11.012.

[30] De la Varga I, Muñoz JF, Bentz DP, Spragg RP, Stutzman PE, Graybeal BA (2018) Grout–concrete interface bond performance: Effect of interface moisture on tensile bond strength and grout microstructure. Constr Build Mater 170:747–756. https://doi.org/10.1016/j.conbuildmat.2018.03.076.

[31] Veludo J, Júlio ENBS, Dias-da-Costa D (2012) Compressive strength of micropile-to-grout connections. Constr Build Mater 26(1):172–179. https://doi.org/10.1016/j.conbuildmat.2011.06.007.

[32] Demircioğlu E, Can G (2025) Identification and evaluation of lean tools, techniques and methods: Pre-construction, construction and post-construction processes. J Constr Eng Manag Innov 8(2):163–184. https://doi.org/10.31462/jcemi.2025.02163184.

[33] Sözen H, Sözer H (2025) Quantifying environmental impacts of residential building lifespans via integrated life cycle assessment and digital modelling techniques. J Constr Eng Manag Innov 8(2):185–208. https://doi.org/10.31462/jcemi.2025.02185208.

[34] Kılıç Bakırhan E, Tuna Kayılı M (2025) Mitigating fit-out waste in rentable offices: The role of flexible design strategies. J Constr Eng Manag Innov 8(4):521–541. https://doi.org/10.31462/jcemi.2025.04521541.